

Adaptive confidence thresholding for semi-supervised monocular depth estimation

Hyesong Choi^{1*}, Hunsang Lee^{2*}, Sunkyung Kim¹, Sunok Kim², Seungryong Kim³, Dongbo Min^{1†}
¹Ewha W. University, ²Yonsei University, ³Korea University,

Abstract

Self-supervised monocular depth estimation has become an appealing solution to the lack of ground truth labels, but its reconstruction loss often produces over-smoothed results across object boundaries and is incapable of handling occlusion explicitly. In this paper, we propose a new approach to leverage *pseudo* ground truth depth maps of stereo images generated from pretrained stereo matching methods. Our method is comprised of three subnetworks; monocular depth network, confidence network, and threshold network. The confidence map of the pseudo ground truth depth map is first estimated to mitigate performance degeneration by inaccurate pseudo depth maps. To cope with the prediction error of the confidence map itself, we also propose to leverage the threshold network that learns the threshold τ in an adaptive manner. The confidence map is thresholded via a differentiable soft-thresholding operator using this truncation boundary τ . The pseudo depth labels filtered out by the *thresholded* confidence map are finally used to supervise the monocular depth network. To apply the proposed method to various training dataset, we introduce the network-wise training strategy that transfers the knowledge learned from one dataset to another. Experimental results demonstrate superior performance to state-of-the-art monocular depth estimation methods. Lastly, we exhibit that the threshold network can also be used to improve the performance of existing confidence estimation approaches.

1 Introduction

Monocular depth estimation, which predicts a dense depth map from a single image, plays an important role in various fields such as scene understanding, robotics, and autonomous driving. This task is heavily underconstrained since a single image may be produced from an infinite number of distinct 3D scenes. Early works on the monocular depth estimation (Eigen, Puhrsch, and Fergus 2014; Li et al. 2015; Cao, Wu, and Shen 2017) are largely based on supervised learning in which the performance largely depends on a huge amount of training data with ground truth depth labels.

Since establishing such a large-scale training data is very costly and labor-intensive, recent approaches rely mostly on

the self-supervised learning regime (Garg et al. 2016; Godard, Mac Aodha, and Brostow 2017; Luo et al. 2018; Godard et al. 2019; Poggi et al. 2020). Instead of using ground truth labels for training the networks, they attempt to leverage the self-supervision from a pair of stereo images or monocular video sequences. They are based on the fact that the geometric structure of a scene can be encoded with the reconstruction loss based on pixel-wise intensity similarities (Garg et al. 2016). This loss function seems to be an appealing alternative to the lack of large-scale ground truth labels, but it often leads to blurry results around depth boundaries and does not consider occluded pixels between two images (Godard, Mac Aodha, and Brostow 2017).

In this paper, we adopt a completely different strategy to resolve the problem caused by insufficient ground truth labels. Instead of relying on the self-supervision using the reconstruction loss across stereo images, we attempt to train the monocular depth estimation networks through *pseudo* depth labels of the stereo images generated from fixed, pretrained stereo matching networks, e.g. (Pang et al. 2017; Chang and Chen 2018). To mitigate performance degeneration by inaccurate pseudo depth labels, we also predict a stereo confidence map ($\in [0, 1]$) indicating the reliability of the pseudo depth labels.

The naive use of the confidence map such as a linear combination (e.g. soft-weighting) with pseudo depth labels, however, may lead to undesired artifacts due to prediction errors in the confidence map itself, when training the monocular depth estimation networks. This may be mitigated by simply truncating the confidence map with a pre-defined threshold (Cho et al. 2019; Tonioni et al. 2019) so that depth values with a low confidence are excluded. However, the empirically-tuned threshold remains fixed for the whole dataset, and still has the risk of inaccurate pseudo depth values being used in the network training. To overcome this limitation, we propose a novel architecture that learns the threshold in an adaptive manner considering image characteristics.

Figure 1 shows the proposed method consisting of monocular depth network, confidence network, and threshold network. To cope with the prediction error of the confidence map itself, the threshold τ is learned from the threshold network. The confidence map is then thresholded by τ using the soft-thresholding operator that is smooth and differen-

*Equal contribution.

†Corresponding author.

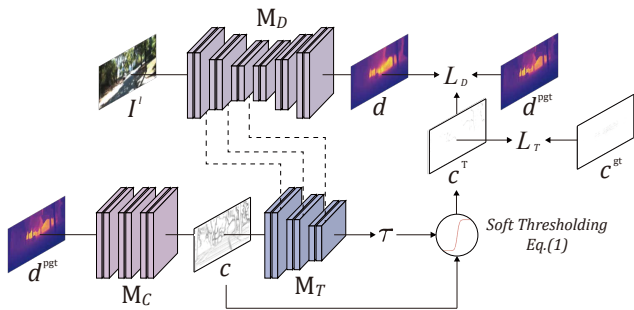


Figure 1: The proposed architecture consisting of monocular depth network M_D , confidence network M_C , and threshold network M_T . Given stereo images, the pseudo ground truth depth maps d^{pgt} of the left image I^l is precomputed using the fixed pretrained stereo matching network. The proposed model training begins with d^{pgt} by computing its confidence map c and the threshold τ through M_C and M_T , respectively. The thresholded confidence map c^T is obtained using the soft-thresholding operation. M_D is finally trained using d^{pgt} filtered out by c^T .

tiable. It is finally used to train the monocular depth network through the depth regression loss function together with the pseudo depth labels.

Our method leverages the sparse ground truth depth map for training the confidence and threshold networks, similar to existing confidence estimation approaches (Poggi and Mattoccia 2016; Park and Yoon 2015; Spyropoulos and Mordohai 2016; Kim et al. 2019), while the monocular depth network uses the pseudo depth labels computed from stereo images. For instance, a set of stereo images and sparse depth maps of 3% density, provided from KITTI dataset (Geiger et al. 2013), can be utilized for training the proposed networks. Thus, our method can be seen as a semi-supervised learning approach. Note that very sparse depth maps, e.g., with 3% density are enough to train the proposed networks.

For the Cityscape dataset (Cordts et al. 2016) with stereo image pairs with no ground truth depth maps, our method can also be applied with a network-wise training strategy. To be specific, the confidence and parameter networks trained with the KITTI dataset are used to train the monocular depth network for the Cityscape dataset. Note that it has been widely reported in literatures (Tosi et al. 2017; Kim et al. 2018; Tonioni et al. 2019) that the confidence network trained with one dataset (e.g. KITTI dataset) works very well on another dataset (e.g. Cityscape or Middlebury datasets). In a similar context, our confidence and threshold networks trained with the KITTI dataset show satisfactory generalization capability for different datasets.

Interestingly, the threshold network can also be beneficial to improving the performance of the confidence estimation approach itself. As shown in Figure 2, the thresholding function controlled by τ attenuates low confidence values to become as close as 0 while amplifying high confidence values to converge to 1, encouraging the confidence to have a bimodal distribution consisting of 0 and 1. Such a binarization operation improves the prediction accuracy of the confi-

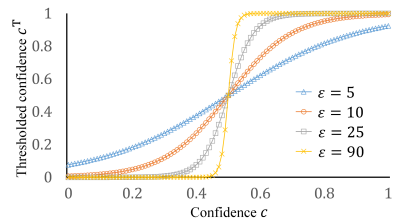


Figure 2: The differential soft-thresholding function in (1). ϵ is a hyperparameter.

dence estimation approach that uses only a sigmoid function to predict the confidence probability.

To sum up, our contribution can be summarized as below.

- We propose a novel framework for monocular depth estimation using the pseudo depth labels in a semi-supervised manner.
- We introduce the threshold network that adaptively learns the threshold of the confidence map for better predicting the reliability of the pseudo depth labels.
- The threshold network can also enhance the prediction accuracy of the confidence estimation method.

2 Related Work

Monocular depth estimation. Eigen *et al.* (2014) initiated the monocular depth estimation through deep networks that regresses a depth map with ground-truth depth information, inspiring numerous approaches based on multi-scale images (Li et al. 2015), up-projection technique (Laina et al. 2016), motion parallax (Ummenhofer et al. 2017), ordinal regression (Fu et al. 2018), and semantic divide-and-conquer (Wang et al. 2020). Despite remarkable performance over classical handcrafted approaches, they rely on abundant and high-quality ground-truth depth maps, which is costly to obtain.

To overcome this limitation, self-supervised learning has been introduced by leveraging other forms of supervision from stereo images and video sequences instead of ground truth depth maps. Garg *et al.* (2016) used the stereo photometric reprojection. Godard *et al.* (2017) further used the left-right consistency between stereo images. Zhou *et al.* (2017) proposed to leverage multi-view synthesis procedure, and this idea was extended using the feature-based warping loss in (Zhan et al. 2018). To take advantages of both supervised and self-supervised learning methods, semi-supervised learning methods have also been presented. Kuznetsov *et al.* (2017) directly combined supervised and unsupervised loss terms. Ji *et al.* (2019) utilizes an image-depth pair discriminator with a small amount of labeled dataset, alleviating the reliance on supervision.

The most related to our work is the methods of Guo *et al.* (2018), Cho *et al.* (2019), and Tonioni *et al.* (2019) in which a stereo matching knowledge is distilled to train a monocular depth network. Since the disparity map estimated by stereo matching inherently contain unreliable ones, they used a stereo confidence to build a pseudo ground-truth disparity map by thresholding the confidence. Guo *et al.* (2018)

used a handcrafted occlusion map sensitive to outliers. Cho *et al.* (2019) used a fixed threshold empirically, but it is ineffective to use the same threshold for all images. Unlike this, Tonioni *et al.* (2019) tried to learn the threshold by using an additional regularization term that allows it to be between 0 and 1, but it is also difficult to learn the appropriate threshold with no explicit supervision on it. In our method, an effective threshold learning is the main contribution.

Stereo confidence estimation. In parallel with an evolution of predicting depth from images, the stereo confidence estimation has also been actively studied. Machine learning approaches (Park and Yoon 2015; Spyropoulos and Morдохай 2016; Kim et al. 2017) relying on shallow classifier, e.g., random tree(), enable one to classify correct and incorrect pixels. Recently, deep convolutional neural networks (CNNs)-based approaches have become a main stream. Various methods have been proposed that use the single- or bimodal input, e.g., disparity (Poggi and Mattocchia 2016), left and right disparities (Seki and Pollefeys 2016), 3D matching cost (Shaked and Wolf 2017), 3D matching cost and disparity (Kim et al. 2018), and disparity and color image (Tosi et al. 2018; Fu and Fard 2018). Kim *et al.* (2019) proposed to make full use of the tri-modal input in conjunction with locally adaptive attention and scale networks, achieving state-of-the-art prediction accuracy. All of these techniques have been used to refine a depth (or disparity) map with a fixed threshold which is set empirically.

3 Proposed Method

3.1 Motivation and Overview

Self-supervised learning for monocular depth estimation has become a prevalent strategy to the problem of insufficient ground truth labels by leveraging other forms of supervision from stereo images and monocular video. Its reconstruction loss, however, often leads to over-smoothed results across object boundaries and is incapable of handling occluded pixels explicitly. We propose a new approach to leverage the *pseudo* depth labels from a pair of stereo images as supervision for monocular depth estimation. Figure 1 presents the overall procedure of the proposed method consisting of three sub-networks; monocular depth estimation network M_D , confidence estimation network M_C , and threshold network M_T . We precompute the pseudo depth labels d^{pgt} of stereo images using the fixed pretrained stereo matching method (Pang et al. 2017).

The proposed model training begins with the precomputed pseudo depth labels d^{pgt} . Their confidence map c is first estimated by the confidence estimation network M_C , aiming at preventing the abuse of erroneous depth values in training the monocular depth network. To take into account the prediction errors of the confidence map itself, we further learn the threshold τ , truncating the confidence map, in an adaptive manner through the threshold network M_T . To make the threshold learning differentiable, we approximate the thresholding operation using τ with a differential function, called soft-thresholding. The thresholded confidence map c^T is obtained via the soft-thresholding by the learned threshold τ . This operation works as trusting the pixel with



(a) Images with high τ values



(b) Images with low τ values

Figure 3: Examples of the estimated threshold τ . CS indicates the Cityscapes dataset. This value becomes higher in images where it is difficult to obtain high-quality pseudo depth labels using stereo matching, and vice versa.

a higher confidence value than a specific τ value. Finally, the monocular depth estimation network M_D is trained using the pseudo depth labels d^{pgt} filtered out by the thresholded confidence map c^T . In the following, more details are presented, including the network architectures, loss functions, and training details.

3.2 Network Architecture

The monocular depth estimation network M_D is based on the encoder-decoder architecture (Ronneberger, Fischer, and Brox 2015). The encoder network consists of the first 13 convolution layers of the VGG network (Simonyan and Zisserman 2014), and the decoder is symmetrical with the encoder. The threshold network M_T resembles the encoder of the monocular depth estimation network. Convolutional features from the encoder of the monocular depth estimation network M_D are concatenated to the threshold network M_T for reflecting image characteristics. For the confidence estimation network M_C , any architectures (Poggi and Mattocchia 2016; Kim et al. 2019; Tosi et al. 2019) for confidence estimation can be used. In our work, the CCNN (Poggi and Mattocchia 2016) is adopted thanks to its simplicity, but more sophisticated models may also be utilized as a backbone.

The estimated confidence map c is modulated by the threshold τ , such that a depth value with a higher confidence value than a specific τ value assumes to be trustworthy. A key issue is how to set τ accordingly which needs to vary depending on the images. This threshold τ should be set low in the image where depth inference is easy, while being set high in the opposite case (see Figure 3). We approximate the thresholding operation with a smooth, differentiable function. The thresholded confidence map c^T is computed using the differentiable soft-thresholding function as follows:

$$c_p^T(\tau) = \frac{1}{1 + e^{-\varepsilon \cdot (c_p - \tau)}}, \quad (1)$$

where p represents a pixel. The slope of the thresholded confidence map c^T is controlled by a hyperparameter ε , which is a positive constant. Figure 2 shows the curvature of the soft-thresholding function according to ε value when $\tau = 0.5$.

The larger ε , the tighter c^T values are mapped to 0 or 1. Note that a too large ε changes the soft-thresholding function too rapidly (e.g. $\varepsilon = 90$), often making it non-differentiable in practice. We set $\varepsilon = 10$ over all experiments.

Figure 3 presents the estimation results of the threshold network for KITTI and Cityscape datasets. The threshold τ becomes higher in images where it is difficult to obtain high-quality pseudo depth labels using stereo matching, and vice versa. This indicates that the threshold network is beneficial to improving the monocular depth network by excluding unreliable depth values of the pseudo ground truth depth map more effectively.

Figure 4 shows the examples of how the monocular depth estimation is gradually improved. Some pixels of the pseudo depth maps are inaccurate to use solely as the supervision for the monocular depth network. By leveraging thresholded confidence map c^T , our method successfully excludes the unconfident pixels from training, producing better results.

3.3 Loss Functions

Depth regression loss The monocular depth network M_D predicts a depth map, which is used for measuring a confidence-guided depth regression loss L_D assisted by the thresholded confidence map c^T , defined as follows:

$$L_D = \frac{1}{Z} \sum_{p \in \Omega} c_p^T(\tau) \cdot |d_p - d_p^{\text{pgt}}|_1, \quad (2)$$

where d and d^{pgt} indicate the predicted depth map and pseudo ground truth depth map, respectively. Ω represents a set of all pixels. The loss is normalized with $Z = \sum c_p^T(\tau)$. We found that training the networks with depth maps tends to produce better results than training with disparity maps, and thus all experiments were conducted on the depth domain. The conversion between disparity and depth maps is straightforward using the focal length and baseline of a stereo camera.

Thresholding loss To train the confidence and threshold networks, we propose to use the sparse ground truth depth data provided by public benchmarks. For instance, we can leverage a set of stereo image pairs and sparse depth maps of 3% density provided in the KITTI dataset. The sparse LiDAR depth maps act as important control points that determine the threshold τ .

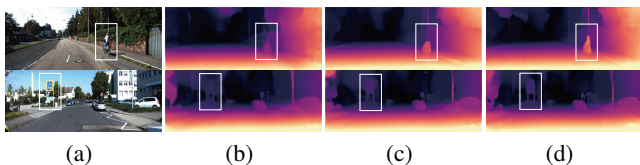


Figure 4: Examples of gradually improved depth results of (a) input image, (b) using our monocular depth network without confidence and threshold networks, (c) using our monocular depth network with confidence network with τ being fixed to 0.3, and (d) using the proposed method.

The loss L_T for the threshold network is defined as follows:

$$L_T = \sum_{p \in \Phi} (c_p^{\text{gt}} \log(c_p^T(\tau)) + (1 - c_p^{\text{gt}}) \log(1 - c_p^T(\tau))), \quad (3)$$

where Φ represents a set of pixels with valid c_p^{gt} . The ground truth c^{gt} of the thresholded confidence map is obtained using the sparse ground truth depth data in a manner similar to existing confidence estimation approaches (Kim et al. 2019; Tonioni et al. 2019). More details on the ground truth confidence map are provided in the supplementary material. As shown in Figure 1, the confidence and threshold networks, M_C and M_T , are trained with (3), whereas the monocular depth network M_D is trained with (2). It is worthy of noting that if the threshold network is trained solely with the loss in (2) using the pseudo depth labels, the threshold τ would often converge to 1 in order to minimize (2).

In (Tonioni et al. 2019), the threshold is also learned to exclude depth values with low confidences in training the networks for monocular depth estimation. It was also reported that when using the depth regression loss only, the threshold τ would converge to 1 for masking out all pixels (Tonioni et al. 2019). Thus, they propose to include an additional regularization term, $-\log(1 - \tau)$, that prevents the threshold τ from approaching 1. Though this term allows τ to be between 0 and 1, the networks do not guarantee to achieve accurate prediction results with no explicit supervision on the threshold τ . Contrastingly, our method attempts to learn the threshold τ using the additional supervision generated by the sparse depth maps, as explained in Figure 1.

Though L_T enables the threshold network to learn τ , both stereo image pairs and corresponding sparse ground truth depth maps are required for training the whole networks. While such training data exists only in a few benchmarks such as the KITTI dataset (e.g., stereo images and LiDAR depth map of 3% density) (Geiger et al. 2013), the Cityscape dataset (Cordts et al. 2016) provides only stereo image pairs with no ground truth depth maps. To address this issue, we propose the network-wise training strategy for training the *incomplete* dataset such as the Cityscape dataset, which will be discussed in the following section.

3.4 Training Details

As explained in Section 3.3, stereo image pairs and corresponding sparse depth maps are required for training our method using (2) and (3), but the Cityscape dataset provides a pair of stereo images only. Interestingly, it has been reported in literatures (Poggi and Mattoccia 2016; Tosi et al. 2018) that the confidence network trained with one dataset (e.g. KITTI dataset) works very well on another dataset (e.g. Cityscape or Middlebury datasets). In addition, the confidence and threshold networks play a role of assisting the monocular depth estimation network by identifying reliable depth values from pseudo ground truth depth maps. Taking these into account, we address this issue by transferring the knowledge learned from one dataset to another through the network-wise training strategy.

When using the *complete* dataset with stereo image pairs

Algorithm 1: The Network-wise Training

Case 1) Stereo images and sparse depth maps, e.g. KITTI/* **Method 1-(a)** */**Output:** Trained parameters of M_D and M_T **Procedure:** Step 1 - 2/* **Method 1-(b)** */**Output:** Trained parameters of M_D , M_C , and M_T **Procedure:** Step 1 - 6

- 1 : Fix M_C with pre-trained confidence network.
- 2 : Train M_D and M_T using L_D and L_T .
- 3 : Fix M_D with the model trained in Step 2.
- 4 : Train M_C and M_T using L_T .
- 5 : Fix M_C and M_T with the models trained in Step 4.
- 6 : Train M_D using L_D .

Case 2) Stereo images only, e.g. Cityscapes/* **Method 2-(a)** */**Output:** Trained parameters of M_D **Procedure:** Step 1 - 2

- 1 : Fix M_C and M_T with pre-trained models of Step 4 in **Case 1**.
 - 2 : Train M_D using L_D
-

and sparse depth maps (e.g. KITTI dataset), the whole networks are trained by minimizing both (2) and (3). Note that very sparse depth maps, e.g., with 3% density are enough to optimize (3). When the *incomplete* dataset with stereo image pairs only (e.g. Cityscape dataset) are given for training, only the monocular depth network is trained via the minimization of (2), with the confidence and threshold networks being frozen with the parameters trained with the complete dataset. Algorithm 1 shows the training procedure for two cases classified according to the presence of the sparse depth maps.

As reported in literatures (Poggi and Mattoccia 2016; Tosi et al. 2018) that the confidence estimation network trained with one dataset (e.g. KITTI dataset) exhibits a good generalization capability for another dataset (e.g. Cityscape or Middlebury datasets), our confidence and threshold networks trained with the KITTI dataset work well for the Cityscape dataset.

We also found that training the whole networks from a scratch at once is challenging due to an imbalanced supervision. For instance, when training with the KITTI dataset, the confidence and threshold networks, M_C and M_T , rely on the *sparse* ground truth depth maps of 3% density, while the monocular depth network M_D leverages the *dense* pseudo ground truth depth maps. Such an imbalanced supervision may make the back-propagation from the monocular depth network M_D overwhelm that of the remaining networks, often leading to unstable network training. To address this issue in the current setup, we propose to split the training procedure for the case 1 of Algorithm 1. The key solution is to separate the monocular depth network M_D and the confidence network M_C . This is because the confidence network M_C infers the confidence map, whose training is rather daunting, while the threshold network M_T inferring the threshold τ is relatively easy to train.

As described in the case 1 of Algorithm 1, the whole net-

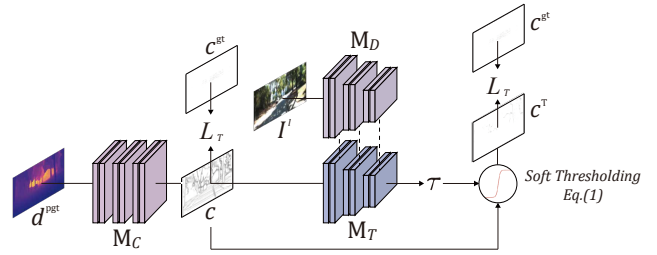


Figure 5: The network architecture for confidence estimation boosted by the soft-thresholding.

works are trained with the following procedures. First, the monocular depth network M_D and the threshold network M_T are trained with the confidence network M_C being frozen with pretrained parameters provided in (Poggi and Mattoccia 2016). Next, the confidence network M_C and the threshold network M_T are trained, while the monocular depth network M_D is frozen with the parameters obtained in the previous step. Finally, the monocular depth network M_D is solely trained with the confidence network M_C and the threshold network M_T being frozen with the parameters obtained in the previous step. We also evaluate the performance for ‘Method 1-(a)’ and ‘Method 1-(b)’. Our code will be publicly available later.

4 Extension to Confidence Estimation

The soft-thresholding attenuates low confidence values to become as close as 0 while amplifying high confidence values to converge to 1. It reduces the number of ambiguous pixels to determine the reliability, for which a confidence value is far from 0 or 1. Such a binarization operation improves the prediction accuracy of the confidence estimation networks.

In this section, we discuss how the soft-thresholding based on the threshold network can improve the prediction accuracy of the confidence estimation approach itself. Figure 5 shows the network architecture for confidence estimation boosted by the soft-thresholding. Similar to Figure 1, the confidence network and threshold network are connected sequentially, and the encoder of the monocular depth network is used so that the color image features are concatenated to the threshold network. One difference is that the same loss function L_T is imposed twice at the confidence network and threshold network, respectively. Also, the loss is measured on the disparity domain, considering that existing confidence estimation networks are trained on the disparity domain. This formulation is the model-agnostic, and any kind of confidence estimation networks can be used here.

5 Experimental results

5.1 Implementation details

The proposed method was implemented in PyTorch with Titan RTX GPU. We trained the whole networks on learning rate of 10^{-4} and batches of 32 images resized to 192×480 for 30 epochs. For depth estimation network, we trained the depth estimation network on the standard 20000 images with

Table 1: Quantitative evaluation for monocular estimation with existing methods on KITTI eigen split dataset. Numbers in bold and underlined represent 1st and 2nd ranking, respectively.

Method	Data	Sup	Lower is better				Accuracy: higher is better		
			Abs Rel	Sqr Rel	RMSE	RMSE log	$\delta < 1.25$	$\delta < 1.25^2$	$\delta < 1.25^3$
Monodepth	S	<i>Self.</i>	0.138	1.186	5.650	0.234	0.813	0.930	0.969
Uncertainty	S	<i>Self.</i>	0.107	0.811	4.796	0.200	0.866	0.952	0.978
MonoResMatch	S	<i>Self.</i>	0.111	0.867	4.714	0.199	0.864	0.954	0.979
Kuznietsov <i>et al.</i>	L+LiDAR	<i>Sup.</i>	0.122	0.763	4.815	0.194	0.845	0.957	0.987
Kuznietsov <i>et al.</i>	S+LiDAR	<i>Semi.</i>	0.113	0.741	4.621	0.189	0.862	0.960	0.986
Monodepth2	S	<i>Self.</i>	0.108	0.842	4.891	0.207	0.866	0.949	0.976
DepthHint	S	<i>Self.</i>	0.102	0.762	4.602	0.189	0.880	0.960	0.981
Guizilini <i>et al.</i>	S+Sem	<i>Self.</i>	0.102	0.698	4.381	0.178	0.896	0.964	0.984
Our Method 1-(a)	L+PGT	<i>Semi.</i>	<u>0.099</u>	<u>0.657</u>	<u>4.289</u>	<u>0.185</u>	<u>0.884</u>	<u>0.962</u>	<u>0.982</u>
Our Method 1-(b)	L+PGT	<i>Semi.</i>	0.098	0.647	4.253	0.186	<u>0.884</u>	0.960	0.981

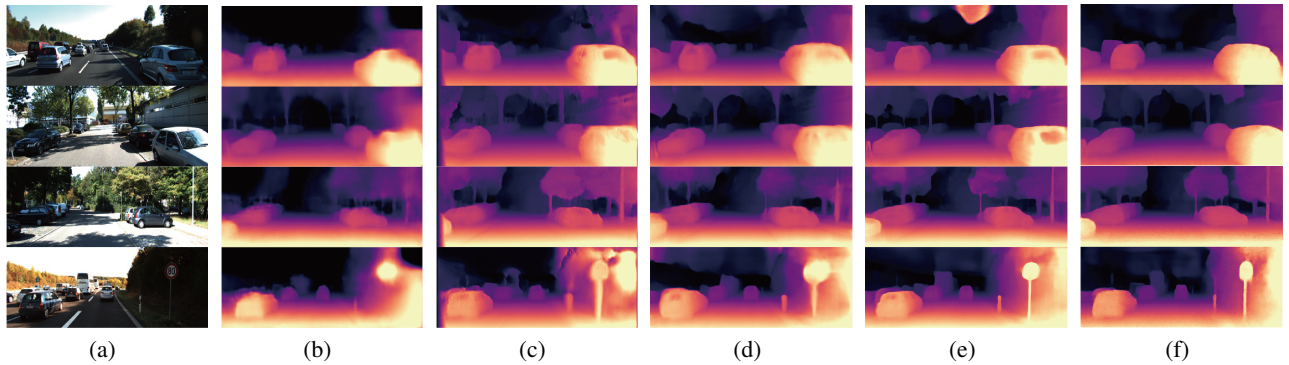


Figure 6: Qualitative evaluation with existing monocular depth estimation methods on the Eigen Split of KITTI dataset: (a) input image, (b) Kuznietsov *et al.* (2017), (c) Monodepth (Godard, Mac Aodha, and Brostow 2017), (d) Monodepth2 (Godard et al. 2019), (e) DepthHint (Watson et al. 2019), and (f) Our Method 1-(b) of Algorithm 1.

sparse LiDAR depth maps of 3% density provided in the KITTI dataset. The performance was measured using five evaluation metrics, ‘RMSE’, ‘RMSE log’, ‘Abs Rel’, ‘Sq. Rel’, and ‘Accuracy’, proposed in Eigen *et al.* (2014). For confidence estimation network, we trained the two confidence estimation methods with 20 out of 194 images provided in KITTI 2012 training dataset (Geiger et al. 2013). The area under the curve (AUC), which is a common metric for confidence estimation approaches, was used (Hu and Mordohai 2012). Due to page limits, some results are provided in supplementary materials.

5.2 Evaluation on monocular depth estimation

KITTI In Table 1, we evaluated the depth estimation performance of our method quantitatively on the KITTI eigen split (Eigen, Puhersch, and Fergus 2014) dataset with setting maximum depth to 80 meters with Gargs crop (Garg et al. 2016). Comprehensive evaluation of the proposed method 1-(a) and 1-(b) of Case 1 described in Algorithm 1 was conducted with Monodepth (Godard, Mac Aodha, and Brostow 2017), Uncertainty (Poggi et al. 2020), MonoResMatch (Tosi et al. 2019), Kuznietsov *et al.* (2017), Monodepth2 (Godard et al. 2019), DepthHint (Watson et al. 2019), Guizilini *et al.* (2020). For the training data, ‘S’ and

‘L’ refers to stereo images and left image respectively. ‘Sem’ is a supervision by models trained with semantic segmentation networks, and ‘PGT’ refers to our proposed pseudo ground truth. Figure 6 shows the qualitative comparison with existing methods on KITTI eigen split dataset. Our methods help to recover complete instances with fine object boundaries.

Cityscapes As the fact that the confidence network trained with one dataset works very well on another dataset, we evaluated the proposed method on the Cityscapes dataset using ‘Method 2-(a)’ of Algorithm 1. Figure 7 shows the qualitative comparison with various methods. Though the pre-trained models are used for the confidence and threshold networks, we outperform others including cutting-edge methods.

5.3 Confidence evaluation

We validated the effectiveness of the threshold network in terms of confidence prediction accuracy by applying it to two confidence estimation approaches, CCNN (Poggi and Mattoccia 2016) and LAFNet (Kim et al. 2019). Refer to the supplementary material for more details on measuring AUC and optimal AUC. We trained the two confidence estimation methods with 20 out of 194 images provided in KITTI 2012

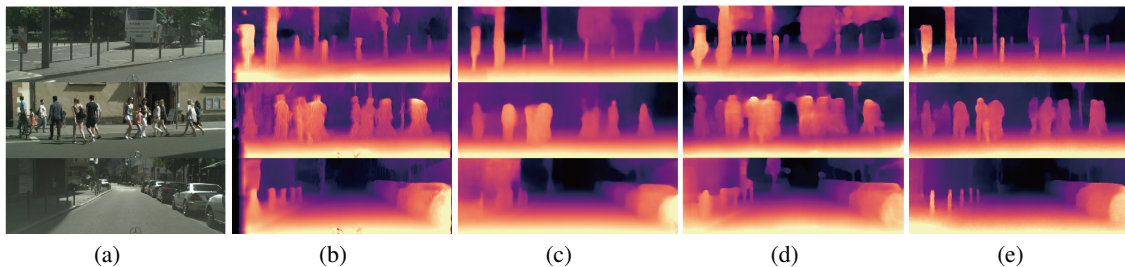


Figure 7: Qualitative evaluation for depth estimation with existing methods on Cityscapes validation dataset. Above figure shows the qualitative results on the 500 validation set of Cityscapes dataset : (a) input image, (b) (Godard, Mac Aodha, and Brostow 2017), (c) (Tosi et al. 2019), (d) (Watson et al. 2019), (e) the proposed method 2-(a) in Algorithm 1.

Table 2: Performance evaluation of confidence estimation for KITTI 2012, KITTI 2015, and Middlebury v3 datasets with two popular stereo matching methods C-SGM (Census-SGM) and MCCNN. AUC values are reported and the lower is the better.

	KITTI 2015	MID 2014
	C-SGM / MCCNN	C-SGM / MCCNN
CCNN	1.868 / 3.190	9.486 / 9.787
CCNN w/ τ	1.720 / 3.525	8.314 / 9.497
LAFNet*	1.797 / 3.051	8.895 / 9.660
LAFNet* w/ τ	1.687 / 3.037	8.988 / 9.456
LAFNet	1.680 / 2.903	8.884 / 9.305
LAFNet w/ τ	1.587 / 2.885	8.680 / 8.622
optimal	0.737 / 2.761	3.887 / 4.985

training dataset(Geiger et al. 2013). Following confidence estimation literatures, input disparity maps used for predicting the confidence maps were obtained using two popular stereo algorithms, ‘Census-SGM’ (Hirschmuller 2005) and ‘MCCNN’ (Žbontar and LeCun 2016).

Table 2 shows objective evaluation results for 200 images of KITTI 2015 dataset (Menze and Geiger 2015) and 15 images of Middlebury v3 dataset (Scharstein et al. 2014). ‘w/ τ ’ denotes the proposed network using the soft-thresholding. LAFNet* denotes the LAFNet (Kim et al. 2019) in which 3D cost volume is not used as an input.

Our results consistently outperform those of original confidence estimation methods, demonstrating the effectiveness of the threshold network. Figure 8 compares the confidence maps of all methods visually. While the original confidence maps contain ambiguous values for which it is difficult to determine whether the depth label is correct, the thresholded confidence map of our method yields more distinct values that are close to 0 or 1. Such a binarization enables the estimated confidence to have similar distribution to ground truth confidence, thus improving the discriminative capability.

5.4 Ablation study

Training procedure We evaluated the ablation experiments to validate the performance gain according to the training procedure of the proposed method. In Table 3, each method indicates that, **B**: the our monocular depth network with-

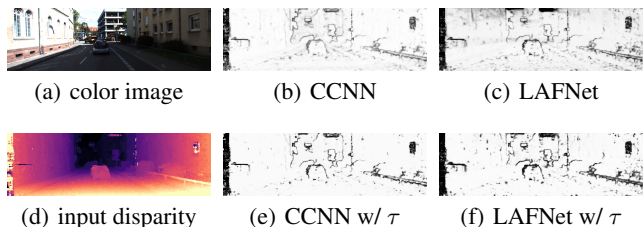


Figure 8: Qualitative results of confidence map on KITTI 2015 dataset using census-SGM.

Table 3: Performance gain according to the training procedure of the proposed method.

	abs	rms	$\delta < 1.25$	$\delta < 1.25^2$	$\delta < 1.25^3$
B	0.108	4.552	0.869	0.957	0.980
B+C	0.102	4.441	0.874	0.959	0.981
MA	0.099	4.289	0.884	0.962	0.982
MB	0.098	4.253	0.884	0.960	0.981

out confidence and threshold networks, **B+C**: the monocular depth network with confidence network with τ being fixed to 0.3, **MA** and **MB**: ‘Method 1-(a)’ and ‘Method 1-(b)’ of Algorithm 1. Compared to **B**, about 10% improvements are achieved in **MB**.

The choice of ε Though the best monocular depth accuracy was achieved when $\varepsilon = 10$, there was no significant change in the performance according to different ε values. More results are available in supplementary materials.

6 Conclusion

In this work, we have proposed a novel framework for monocular depth estimation based on semi-supervised learning. Instead of relying on the self-supervision using the reconstruction loss across stereo images, we proposed to use pseudo depth labels generated by pretrained stereo matching methods. The confidence map is used to exclude erroneous depth values within the pseudo depth labels. The prediction errors in the confidence map are further suppressed by making use of the soft-thresholding based on the threshold learning. The proposed framework has shown the impressive performance over state-of-the-arts on several benchmarks. It was also shown that the threshold learning can also boost the prediction accuracy of existing confidence approaches.

As future work, we will study the possibility of applying the soft-thresholding to various tasks based on binary prediction.

References

- Cao, Y.; Wu, Z.; and Shen, C. 2017. Estimating depth from monocular images as classification using deep fully convolutional residual networks. *IEEE Transactions on Circuits and Systems for Video Technology* 28(11): 3174–3182.
- Chang, J.-R.; and Chen, Y.-S. 2018. Pyramid stereo matching network. In *Proceedings of the IEEE Conference on Computer Vision and Pattern Recognition*, 5410–5418.
- Cho, J.; Min, D.; Kim, Y.; and Sohn, K. 2019. A Large RGB-D Dataset for Semi-supervised Monocular Depth Estimation. *arXiv preprint arXiv:1904.10230*.
- Cordts, M.; Omran, M.; Ramos, S.; Rehfeld, T.; Enzweiler, M.; Benenson, R.; Franke, U.; Roth, S.; and Schiele, B. 2016. The cityscapes dataset for semantic urban scene understanding. In *Proceedings of the IEEE conference on computer vision and pattern recognition*, 3213–3223.
- Eigen, D.; Puhersch, C.; and Fergus, R. 2014. Depth map prediction from a single image using a multi-scale deep network. In *Advances in neural information processing systems*, 2366–2374.
- Fu, H.; Gong, M.; Wang, C.; Batmanghelich, K.; and Tao, D. 2018. Deep ordinal regression network for monocular depth estimation. In *Proceedings of the IEEE Conference on Computer Vision and Pattern Recognition*, 2002–2011.
- Fu, Z.; and Fard, M. A. 2018. Learning confidence measures by multi-modal convolutional neural networks. In *2018 IEEE Winter Conference on Applications of Computer Vision (WACV)*, 1321–1330. IEEE.
- Garg, R.; Bg, V. K.; Carneiro, G.; and Reid, I. 2016. Un-supervised cnn for single view depth estimation: Geometry to the rescue. In *European conference on computer vision*, 740–756. Springer.
- Geiger, A.; Lenz, P.; Stiller, C.; and Urtasun, R. 2013. Vision meets robotics: The kitti dataset. *The International Journal of Robotics Research* 32(11): 1231–1237.
- Godard, C.; Mac Aodha, O.; and Brostow, G. J. 2017. Unsupervised monocular depth estimation with left-right consistency. In *Proceedings of the IEEE Conference on Computer Vision and Pattern Recognition*, 270–279.
- Godard, C.; Mac Aodha, O.; Firman, M.; and Brostow, G. J. 2019. Digging into self-supervised monocular depth estimation. In *Proceedings of the IEEE international conference on computer vision*, 3828–3838.
- Guizilini, V.; Hou, R.; Li, J.; Ambrus, R.; and Gaidon, A. 2020. Semantically-Guided Representation Learning for Self-Supervised Monocular Depth. *arXiv preprint arXiv:2002.12319*.
- Guo, X.; Li, H.; Yi, S.; Ren, J.; and Wang, X. 2018. Learning monocular depth by distilling cross-domain stereo networks. In *Proceedings of the European Conference on Computer Vision (ECCV)*, 484–500.
- Hirschmuller, H. 2005. Accurate and efficient stereo processing by semi-global matching and mutual information. In *2005 IEEE Computer Society Conference on Computer Vision and Pattern Recognition (CVPR'05)*, volume 2, 807–814. IEEE.
- Hu, X.; and Mordohai, P. 2012. A quantitative evaluation of confidence measures for stereo vision. *IEEE transactions on pattern analysis and machine intelligence* 34(11): 2121–2133.
- Ji, R.; Li, K.; Wang, Y.; Sun, X.; Guo, F.; Guo, X.; Wu, Y.; Huang, F.; and Luo, J. 2019. Semi-supervised adversarial monocular depth estimation. *IEEE transactions on pattern analysis and machine intelligence*.
- Kim, S.; Kim, S.; Min, D.; and Sohn, K. 2019. Laf-net: Locally adaptive fusion networks for stereo confidence estimation. In *Proceedings of the IEEE Conference on Computer Vision and Pattern Recognition*, 205–214.
- Kim, S.; Min, D.; Kim, S.; and Sohn, K. 2017. Feature augmentation for learning confidence measure in stereo matching. *IEEE Transactions on Image Processing* 26(12): 6019–6033.
- Kim, S.; Min, D.; Kim, S.; and Sohn, K. 2018. Unified confidence estimation networks for robust stereo matching. *IEEE Transactions on Image Processing* 28(3): 1299–1313.
- Kuznetsov, Y.; Stuckler, J.; and Leibe, B. 2017. Semi-supervised deep learning for monocular depth map prediction. In *Proceedings of the IEEE conference on computer vision and pattern recognition*, 6647–6655.
- Laina, I.; Ruppel, C.; Belagiannis, V.; Tombari, F.; and Navab, N. 2016. Deeper depth prediction with fully convolutional residual networks. In *2016 Fourth international conference on 3D vision (3DV)*, 239–248. IEEE.
- Li, B.; Shen, C.; Dai, Y.; Van Den Hengel, A.; and He, M. 2015. Depth and surface normal estimation from monocular images using regression on deep features and hierarchical crfs. In *Proceedings of the IEEE conference on computer vision and pattern recognition*, 1119–1127.
- Luo, Y.; Ren, J.; Lin, M.; Pang, J.; Sun, W.; Li, H.; and Lin, L. 2018. Single view stereo matching. In *Proceedings of the IEEE Conference on Computer Vision and Pattern Recognition*, 155–163.
- Menze, M.; and Geiger, A. 2015. Object scene flow for autonomous vehicles. In *Proceedings of the IEEE conference on computer vision and pattern recognition*, 3061–3070.
- Pang, J.; Sun, W.; Ren, J. S.; Yang, C.; and Yan, Q. 2017. Cascade residual learning: A two-stage convolutional neural network for stereo matching. In *Proceedings of the IEEE International Conference on Computer Vision Workshops*, 887–895.
- Park, M.-G.; and Yoon, K.-J. 2015. Leveraging stereo matching with learning-based confidence measures. In *Proceedings of the IEEE Conference on Computer Vision and Pattern Recognition*, 101–109.

- Poggi, M.; Aleotti, F.; Tosi, F.; and Mattoccia, S. 2020. On the uncertainty of self-supervised monocular depth estimation. In *Proceedings of the IEEE/CVF Conference on Computer Vision and Pattern Recognition*, 3227–3237.
- Poggi, M.; and Mattoccia, S. 2016. Learning from scratch a confidence measure. In *BMVC*.
- Ronneberger, O.; Fischer, P.; and Brox, T. 2015. U-net: Convolutional networks for biomedical image segmentation. In *International Conference on Medical image computing and computer-assisted intervention*, 234–241. Springer.
- Scharstein, D.; Hirschmüller, H.; Kitajima, Y.; Krathwohl, G.; Nešić, N.; Wang, X.; and Westling, P. 2014. High-resolution stereo datasets with subpixel-accurate ground truth. In *German conference on pattern recognition*, 31–42. Springer.
- Seki, A.; and Pollefeys, M. 2016. Patch Based Confidence Prediction for Dense Disparity Map. In *BMVC*, volume 2, 4.
- Shaked, A.; and Wolf, L. 2017. Improved stereo matching with constant highway networks and reflective confidence learning. In *Proceedings of the IEEE Conference on Computer Vision and Pattern Recognition*, 4641–4650.
- Simonyan, K.; and Zisserman, A. 2014. Very deep convolutional networks for large-scale image recognition. *arXiv preprint arXiv:1409.1556* .
- Spyropoulos, A.; and Mordohai, P. 2016. Correctness prediction, accuracy improvement and generalization of stereo matching using supervised learning. *International Journal of Computer Vision* 118(3): 300–318.
- Tonioni, A.; Poggi, M.; Mattoccia, S.; and Di Stefano, L. 2019. Unsupervised domain adaptation for depth prediction from images. *IEEE transactions on pattern analysis and machine intelligence* .
- Tosi, F.; Aleotti, F.; Poggi, M.; and Mattoccia, S. 2019. Learning monocular depth estimation infusing traditional stereo knowledge. In *Proceedings of the IEEE Conference on Computer Vision and Pattern Recognition*, 9799–9809.
- Tosi, F.; Poggi, M.; Benincasa, A.; and Mattoccia, S. 2018. Beyond local reasoning for stereo confidence estimation with deep learning. In *Proceedings of the European Conference on Computer Vision (ECCV)*, 319–334.
- Tosi, F.; Poggi, M.; Mattoccia, S.; Tonioni, A.; and di Stefano, L. 2017. Learning confidence measures in the wild. In *BMVC*.
- Ummenhofer, B.; Zhou, H.; Uhrig, J.; Mayer, N.; Ilg, E.; Dosovitskiy, A.; and Brox, T. 2017. Demon: Depth and motion network for learning monocular stereo. In *Proceedings of the IEEE Conference on Computer Vision and Pattern Recognition*, 5038–5047.
- Wang, L.; Zhang, J.; Wang, O.; Lin, Z.; and Lu, H. 2020. SDC-Depth: Semantic Divide-and-Conquer Network for Monocular Depth Estimation. In *Proceedings of the IEEE/CVF Conference on Computer Vision and Pattern Recognition*, 541–550.
- Watson, J.; Firman, M.; Brostow, G. J.; and Turmukhambetov, D. 2019. Self-supervised monocular depth hints. In *Proceedings of the IEEE International Conference on Computer Vision*, 2162–2171.
- Žbontar, J.; and LeCun, Y. 2016. Stereo matching by training a convolutional neural network to compare image patches. *The journal of machine learning research* 17(1): 2287–2318.
- Zhan, H.; Garg, R.; Saroj Weerasekera, C.; Li, K.; Agarwal, H.; and Reid, I. 2018. Unsupervised learning of monocular depth estimation and visual odometry with deep feature reconstruction. In *Proceedings of the IEEE Conference on Computer Vision and Pattern Recognition*, 340–349.
- Zhou, T.; Brown, M.; Snavely, N.; and Lowe, D. G. 2017. Unsupervised learning of depth and ego-motion from video. In *Proceedings of the IEEE Conference on Computer Vision and Pattern Recognition*, 1851–1858.

Adaptive confidence thresholding for semi-supervised monocular depth estimation - Supplementary material

Hyesong Choi^{1*}, Hunsang Lee^{2*}, Sunkyung Kim¹, Sunok Kim², Seungryong Kim³, Dongbo Min^{1†}
¹Ewha W. University, ²Yonsei University, ³Korea University,

In this document, we provide more comprehensive results not provided in the original manuscript due to the page limit as below.

- Qualitative evaluation for monocular depth estimation with state-of-the-arts on KITTI and Cityscapes datasets (Section 1.2 and 1.3)
- Quantitative evaluation for monocular depth estimation using improved ground truth depth maps (Uhrig et al. 2017) on KITTI dataset (Section 1.4)
- Performance analysis according to a hyperparameter ϵ used in the soft-thresholding function (Section 1.5)
- Ground truth confidence map and evaluation metric used in the confidence estimation (Section 2)
- Qualitative results for confidence estimation with state-of-the-arts on KITTI dataset (Section 2)

1 Monocular depth estimation results

This section provides more results for comparative study with state-of-the-art methods in terms of monocular depth accuracy.

1.1 Evaluation metrics

In order to evaluate the depth estimation performance, same as the original manuscript, five commonly-used evaluation metrics proposed in (Eigen, Puhrsch, and Fergus 2014) were adopted as follows:

- Abs Rel = $\frac{1}{|\Omega|} \sum_{p \in \Omega} \frac{|d_p - d_p^{\text{gt}}|}{d_p^{\text{gt}}}$
- Sq Rel = $\frac{1}{|\Omega|} \sum_{p \in \Omega} \frac{(d_p - d_p^{\text{gt}})^2}{d_p^{\text{gt}}}$
- RMSE = $\sqrt{\frac{1}{|\Omega|} \sum_{p \in \Omega} (d_p - d_p^{\text{gt}})^2}$
- RMSE log = $\sqrt{\frac{1}{|\Omega|} \sum_{p \in \Omega} (\log(d_p) - \log(d_p^{\text{gt}}))^2}$
- $\delta < 1.25^n = \% \text{ of } d_p \text{ s.t. } \delta = \max\left(\frac{d_p}{d_p^{\text{gt}}}, \frac{d_p^{\text{gt}}}{d_p}\right) < 1.25^n$
for $n = 1, 2, 3$,

*Equal contribution.

†Corresponding author.

where d_p and d_p^{gt} indicate the estimated depth map and ground truth depth map at a pixel p , respectively. Ω represents a set of valid pixels.

1.2 Qualitative evaluation on KITTI

Figure 1 shows the qualitative evaluation with existing monocular depth estimation methods on the Eigen Split (Eigen, Puhrsch, and Fergus 2014) of KITTI dataset. We compared our results with (b) Kuznietsov *et al.* (Kuznietsov, Stuckler, and Leibe 2017), (c) Monodepth (Godard, Mac Aodha, and Brostow 2017), (d) Monodepth2 (Godard et al. 2019), (e) DepthHint (Watson et al. 2019), and (f) Our ‘Method 1-(b)’ of Algorithm 1 in the submitted manuscript. Compared to other results, our method predicts instances very well without holes or distortions while recovering fine object boundaries. Additionally, our method is capable of predicting thin objects precisely.

1.3 Qualitative evaluation on Cityscapes

Figure 2 shows the qualitative results on Cityscapes dataset (Cordts et al. 2016). We compared our results with three existing methods: (b) (Godard, Mac Aodha, and Brostow 2017), (c) (Tosi et al. 2019), (d) (Watson et al. 2019) and (e) the proposed ‘Method 2-(a)’ of Algorithm 1 in the original manuscript. Similar to KITTI results, our method is remarkable at predicting fine details with no distortions at all instances and recovering thin objects that appear frequently in the Cityscapes dataset, whereas other methods often fail to predict accurate depth values at these regions.

1.4 Quantitative evaluation on KITTI with improved ground truth depth maps

To strengthen credibility to quantitative evaluation, we also measured the monocular depth accuracy by using 652 test frames with the improved ground truth depth maps made available in (Uhrig et al. 2017) for KITTI Eigen split dataset (Eigen, Puhrsch, and Fergus 2014). The improved ground truth maps are high quality depth maps generated by accumulating LiDAR point clouds from 5 consecutive frames.

Table 1 shows the quantitative evaluation with existing methods on the KITTI Eigen split dataset using the improved ground truth depth maps (Uhrig et al. 2017). We compared our results with ‘SfMLeaner’ (Zhou et al. 2017), ‘Vid2Depth’ (Mahjourian, Wicke, and Angelova 2018),

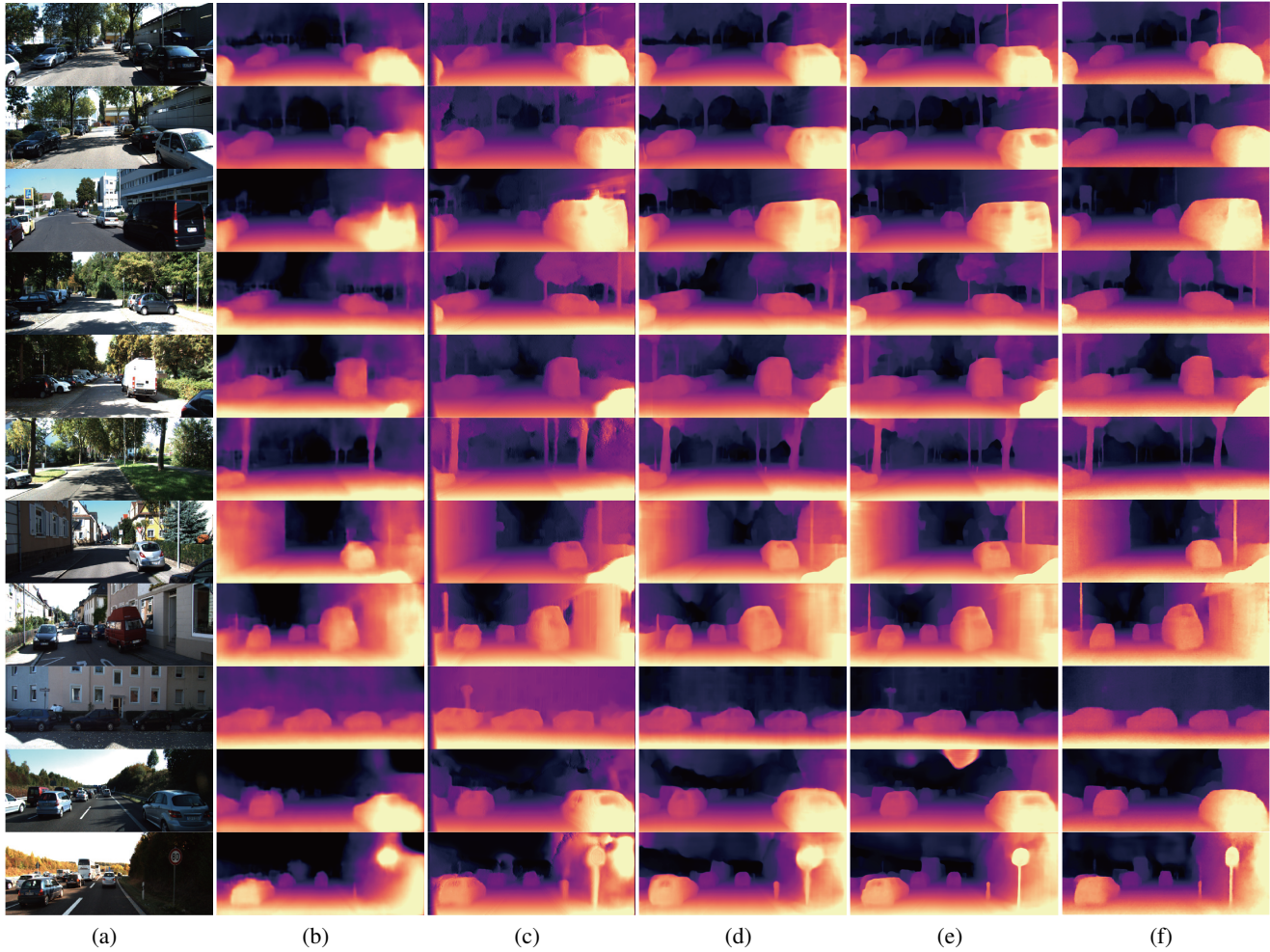


Figure 1: Qualitative evaluation with existing monocular depth estimation methods on the Eigen split (Eigen, Puhrsch, and Fergus 2014) of KITTI dataset: (a) input image, (b) Kuznetsov *et al.* (Kuznetsov, Stuckler, and Leibe 2017), (c) Monodepth (Godard, Mac Aodha, and Brostow 2017), (d) Monodepth2 (Godard et al. 2019), (e) DepthHint (Watson et al. 2019), and (f) the proposed ‘Method 1-(b)’ of Algorithm 1 in the submitted manuscript. Compared to other results, our method predicts instances very well without holes or distortions while recovering fine object boundaries. Additionally, our method is capable of predicting thin instances precisely.

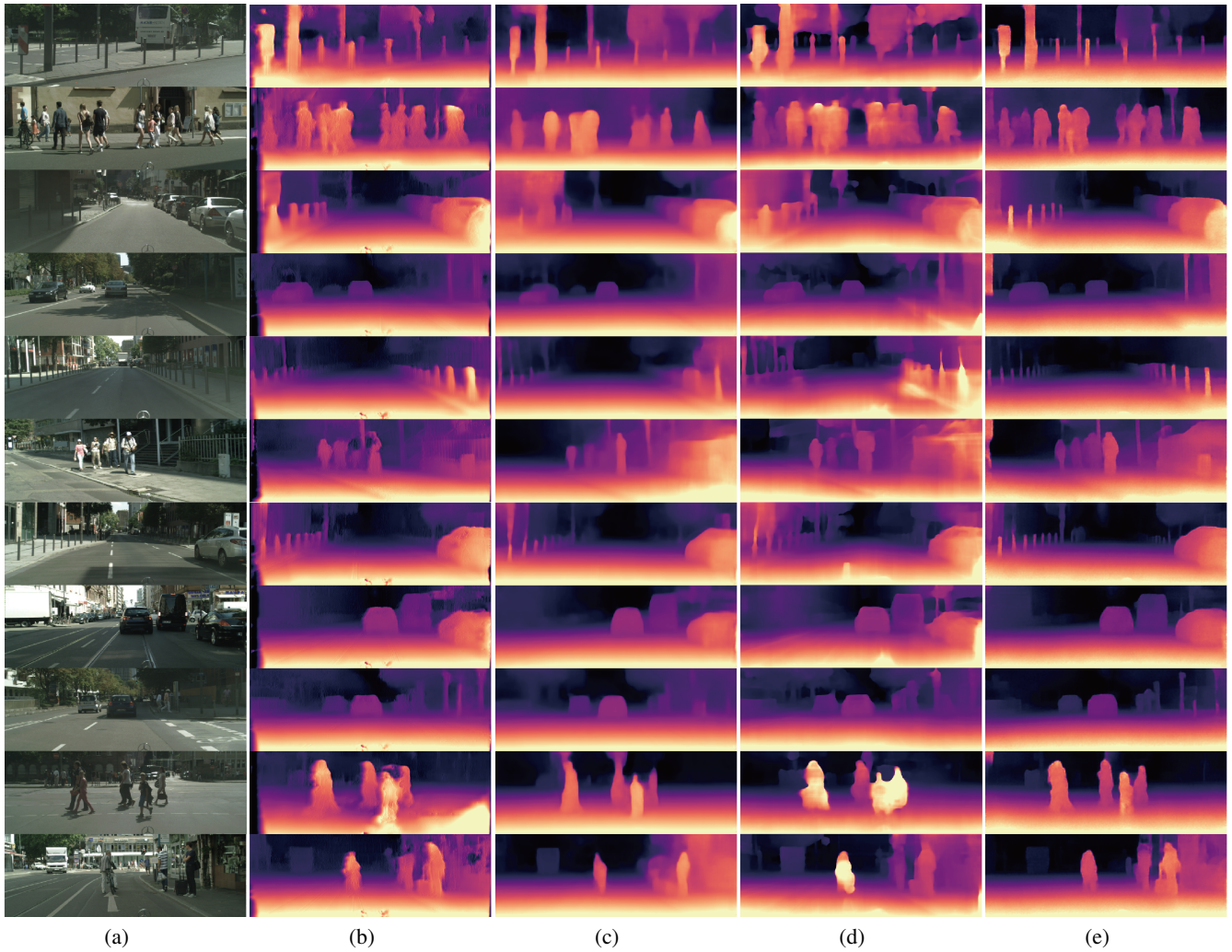


Figure 2: Qualitative evaluation for depth estimation with existing methods on Cityscapes validation dataset: (a) input image, (b) (Godard, Mac Aodha, and Brostow 2017), (c) (Tosi et al. 2019), (d) (Watson et al. 2019) and (e) the proposed ‘Method 2-(a)’ of Algorithm 1 in the original manuscript. Similar to KITTI results, our method is remarkable at predicting fine details with no distortions at all instances and recovering thin objects that appear frequently in the Cityscapes dataset, whereas other methods often fail to predict accurate depth values at these regions.

Table 1: Quantitative evaluation for monocular depth estimation with existing methods on KITTI Eigen split dataset (Eigen, Puhrsch, and Fergus 2014) with improved ground truth depth maps (Uhrig et al. 2017). Numbers in bold and underlined represent 1st and 2nd ranking, respectively. For data, V refers to monocular video, S refers to Stereo and L+PGT refers to training with monocular image and pseudo ground truth.

Method	Data	Lower is better				Accuracy: higher is better		
		Abs Rel	Sqr Rel	RMSE	RMSE log	$\delta < 1.25$	$\delta < 1.25^2$	$\delta < 1.25^3$
SfMLeaner	V	0.176	1.532	6.129	0.244	0.758	0.921	0.971
Vid2Depth	V	0.134	0.983	5.501	0.203	0.827	0.944	0.981
DDVO	V	0.126	0.866	4.932	0.185	0.851	0.958	0.986
EPC++	V	0.120	0.789	4.755	0.177	0.856	0.961	0.987
Monodepth2	V	0.090	0.545	3.942	0.137	0.914	0.983	0.995
Uncertainty (Boot+Log)	S	0.085	0.511	3.777	0.137	0.913	0.980	0.994
Uncertainty (Boot+Self)	S	0.085	0.510	3.792	0.135	0.914	0.981	0.994
Uncertainty (Snap+Log)	S	0.084	0.529	3.833	0.138	0.914	0.980	0.994
Uncertainty (Snap+Self)	S	0.086	0.532	3.858	0.138	0.912	0.980	0.994
PackNet-SfM	V	0.078	0.420	3.485	0.121	0.931	0.986	<u>0.996</u>
UnRectDepthNet	V	0.081	0.414	3.412	0.117	0.926	<u>0.987</u>	<u>0.996</u>
Our Method 1-(a)	L+PGT	<u>0.079</u>	<u>0.364</u>	<u>3.212</u>	<u>0.120</u>	0.931	0.988	0.997
Our Method 1-(b)	L+PGT	0.078	0.357	3.203	<u>0.120</u>	<u>0.930</u>	<u>0.987</u>	<u>0.996</u>

Table 2: Quantitative depth estimation result according to ε value evaluated on KITTI Eigen split (Eigen, Puhrsch, and Fergus 2014) raw dataset.

ε	Abs Rel	Sqr Rel	RMSE	RMSE log	$\delta < 1.25$	$\delta < 1.25^2$	$\delta < 1.25^3$
10	0.098	0.647	4.253	0.186	0.884	0.960	0.981
30	0.101	0.650	4.283	0.188	0.881	0.959	0.980
50	0.100	0.645	4.265	0.188	0.882	0.959	0.980

‘DDVO’ (Wang et al. 2018), ‘EPC++’ (Luo et al. 2019), ‘Monodepth2’ (Godard et al. 2019), ‘Uncertainty’ (Poggi et al. 2020), ‘PackNet-SfM’ (Guizilini et al. 2020), and ‘UnRectDepthNet’ (Kumar et al. 2020). These methods employed the monocular video as supervision except for ‘Uncertainty’ using stereo image pairs. Our methods produce competitive performance compared to other methods.

1.5 Choice of ε value

We set $\varepsilon = 10$ for the differentiable soft-thresholding function in (1) of the original manuscript. Table 2 shows the quantitative results according to ε on the KITTI Eigen split (Eigen, Puhrsch, and Fergus 2014) raw dataset. Though the best accuracy was achieved with $\varepsilon = 10$, no significant change was observed depending on varying ε .

2 Confidence estimation results

To train the confidence network, the ground truth confidence map is required as supervision. Following existing confidence estimation approaches (Poggi and Mattoccia 2016; Kim et al. 2019), the ground truth confidence map c_p^{gt} was computed by using an absolute difference between the ground truth disparity map and the input disparity map, whose confidence is estimated in the confidence network, called the pseudo ground truth disparity map in our work.

$$c_p^{\text{gt}} = \begin{cases} 1, & \text{if } |d_p - d_p^{\text{pgt}}| \leq \rho. \\ 0, & \text{otherwise.} \end{cases} \quad (1)$$

The threshold value ρ is set to 3 for KITTI (Menze and Geiger 2015) and 1 for Middlebury (Scharstein et al. 2014).

The area under the curve (AUC) (Hu and Mordohai 2012) was used for evaluating the performance of estimated confidence maps. The receiver operating characteristic (ROC) curve is first computed by sorting disparity pixels in a decreasing order of confidence and sequentially sampling high confidence disparity pixels. It computes the error rate indicating the percentage of pixels with a difference larger than ρ from ground truth disparity. Then, AUC is computed by integral of the ROC curve. The optimal AUC is computed according to the fact that the error rate ζ is ideally 0 when sampling the first $(1 - \zeta)$ pixels (Hu and Mordohai 2012), which is equal to

$$AUC_{\text{opt}} = \int_{1-\zeta}^1 \frac{x - (1 - \zeta)}{x} dx = \zeta + (1 - \zeta) \ln 1 - \zeta. \quad (2)$$

Figure 3 shows the qualitative results of confidence map evaluated on KITTI 2015 dataset (Menze and Geiger 2015). Input disparity maps used for confidence estimation were obtained by Census-SGM (Hirschmuller 2005). The estimated confidence maps for each input disparity map are displayed every two rows. The top and bottom of two rows indicate: (a) color image and input disparity image, (b) CCNN (Poggi and Mattoccia 2016) and CCNN w/ τ , (c) LAFNet*(Kim et al. 2019) and LAFNet* w/ τ and (d) LAFNet and LAFNet w/ τ . ‘w/ τ ’ denotes the thresh-

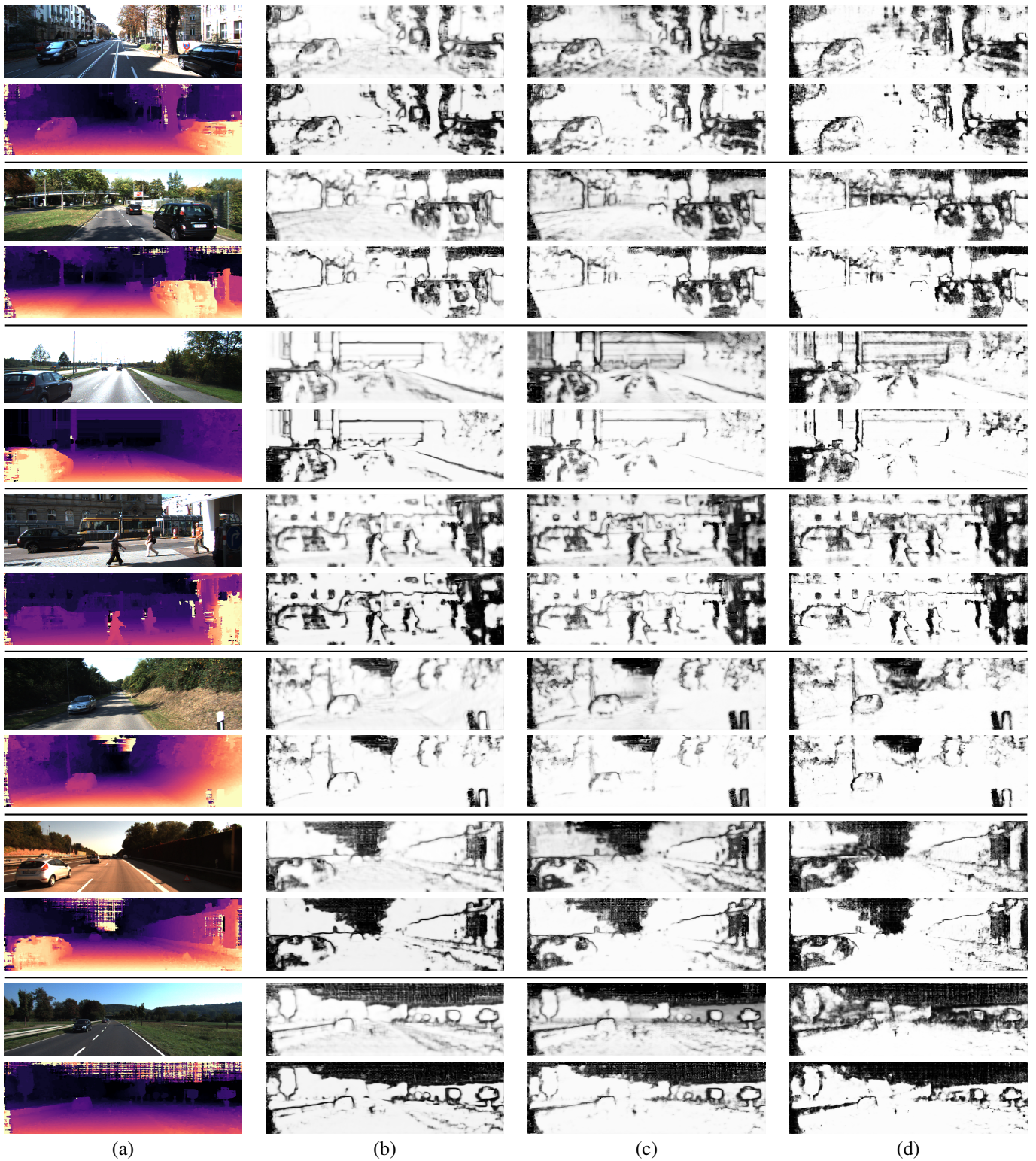


Figure 3: Qualitative evaluation for confidence estimation on KITTI 2015 dataset (Menze and Geiger 2015): Input disparity maps used for confidence estimation were obtained by Census-SGM (Hirschmuller 2005). The estimated confidence maps for each input disparity map are displayed every two rows. The top and bottom of two rows indicate: (a) color image and input disparity image, (b) CCNN (Poggi and Mattoccia 2016) and CCNN w/τ , (c) LAFNet*(Kim et al. 2019) and LAFNet* w/τ and (d) LAFNet and LAFNet w/τ . ‘ w/τ ’ denotes the proposed network using the soft-thresholding. LAFNet* denotes the LAFNet (Kim et al. 2019) in which 3D cost volume is not used as an input.

olded confidence map obtained using the soft-thresholding. LAFNet* denotes the LAFNet (Kim et al. 2019) in which 3D cost volume is not used as an input. As shown in Figure 3, the proposed thresholded confidence maps contain fewer ambiguous values than the original confidence maps.

References

- Cordts, M.; Omran, M.; Ramos, S.; Rehfeld, T.; Enzweiler, M.; Benenson, R.; Franke, U.; Roth, S.; and Schiele, B. 2016. The cityscapes dataset for semantic urban scene understanding. In *Proceedings of the IEEE conference on computer vision and pattern recognition*, 3213–3223.
- Eigen, D.; Puhersch, C.; and Fergus, R. 2014. Depth map prediction from a single image using a multi-scale deep network. In *Advances in neural information processing systems*, 2366–2374.
- Godard, C.; Mac Aodha, O.; and Brostow, G. J. 2017. Unsupervised monocular depth estimation with left-right consistency. In *Proceedings of the IEEE Conference on Computer Vision and Pattern Recognition*, 270–279.
- Godard, C.; Mac Aodha, O.; Firman, M.; and Brostow, G. J. 2019. Digging into self-supervised monocular depth estimation. In *Proceedings of the IEEE international conference on computer vision*, 3828–3838.
- Guizilini, V.; Ambrus, R.; Pillai, S.; Raventos, A.; and Gaidon, A. 2020. 3D Packing for Self-Supervised Monocular Depth Estimation. In *Proceedings of the IEEE/CVF Conference on Computer Vision and Pattern Recognition*, 2485–2494.
- Hirschmuller, H. 2005. Accurate and efficient stereo processing by semi-global matching and mutual information. In *2005 IEEE Computer Society Conference on Computer Vision and Pattern Recognition (CVPR'05)*, volume 2, 807–814. IEEE.
- Hu, X.; and Mordohai, P. 2012. A quantitative evaluation of confidence measures for stereo vision. *IEEE transactions on pattern analysis and machine intelligence* 34(11): 2121–2133.
- Kim, S.; Kim, S.; Min, D.; and Sohn, K. 2019. Laf-net: Locally adaptive fusion networks for stereo confidence estimation. In *Proceedings of the IEEE Conference on Computer Vision and Pattern Recognition*, 205–214.
- Kumar, V. R.; Yogamani, S.; Bach, M.; Witt, C.; Milz, S.; and Mader, P. 2020. UnRectDepthNet: Self-Supervised Monocular Depth Estimation using a Generic Framework for Handling Common Camera Distortion Models. *arXiv preprint arXiv:2007.06676*.
- Kuznetsov, Y.; Stuckler, J.; and Leibe, B. 2017. Semi-supervised deep learning for monocular depth map prediction. In *Proceedings of the IEEE conference on computer vision and pattern recognition*, 6647–6655.
- Luo, C.; Yang, Z.; Wang, P.; Wang, Y.; Xu, W.; Nevatia, R.; and Yuille, A. 2019. Every pixel counts++: Joint learning of geometry and motion with 3d holistic understanding. *IEEE transactions on pattern analysis and machine intelligence*.
- Mahjourian, R.; Wicke, M.; and Angelova, A. 2018. Unsupervised learning of depth and ego-motion from monocular video using 3d geometric constraints. In *Proceedings of the IEEE Conference on Computer Vision and Pattern Recognition*, 5667–5675.
- Menze, M.; and Geiger, A. 2015. Object scene flow for autonomous vehicles. In *Proceedings of the IEEE conference on computer vision and pattern recognition*, 3061–3070.
- Poggi, M.; Aleotti, F.; Tosi, F.; and Mattoccia, S. 2020. On the uncertainty of self-supervised monocular depth estimation. In *Proceedings of the IEEE/CVF Conference on Computer Vision and Pattern Recognition*, 3227–3237.
- Poggi, M.; and Mattoccia, S. 2016. Learning from scratch a confidence measure. In *BMVC*.
- Scharstein, D.; Hirschmüller, H.; Kitajima, Y.; Krathwohl, G.; Nešić, N.; Wang, X.; and Westling, P. 2014. High-resolution stereo datasets with subpixel-accurate ground truth. In *German conference on pattern recognition*, 31–42. Springer.
- Tosi, F.; Aleotti, F.; Poggi, M.; and Mattoccia, S. 2019. Learning monocular depth estimation infusing traditional stereo knowledge. In *Proceedings of the IEEE Conference on Computer Vision and Pattern Recognition*, 9799–9809.
- Uhrig, J.; Schneider, N.; Schneider, L.; Franke, U.; Brox, T.; and Geiger, A. 2017. Sparsity invariant cnns. In *2017 international conference on 3D Vision (3DV)*, 11–20. IEEE.
- Wang, C.; Miguel Buenaposada, J.; Zhu, R.; and Lucey, S. 2018. Learning depth from monocular videos using direct methods. In *Proceedings of the IEEE Conference on Computer Vision and Pattern Recognition*, 2022–2030.
- Watson, J.; Firman, M.; Brostow, G. J.; and Turmukhambetov, D. 2019. Self-supervised monocular depth hints. In *Proceedings of the IEEE International Conference on Computer Vision*, 2162–2171.
- Zhou, T.; Brown, M.; Snavely, N.; and Lowe, D. G. 2017. Unsupervised learning of depth and ego-motion from video. In *Proceedings of the IEEE Conference on Computer Vision and Pattern Recognition*, 1851–1858.